

UC Irvine

UC Irvine Previously Published Works

Title

Interference enhancement in spectral domain interferometric measurements on transparent plate

Permalink

<https://escholarship.org/uc/item/2gd7f979>

Journal

Applied Optics, 53(26)

ISSN

1559-128X

Authors

Zhang, K
Tao, L
Cheng, W
[et al.](#)

Publication Date

2014-09-10

DOI

10.1364/AO.53.005906

Copyright Information

This work is made available under the terms of a Creative Commons Attribution License, available at <https://creativecommons.org/licenses/by/4.0/>

Peer reviewed

Interference enhancement in spectral domain interferometric measurements on transparent plate

Ke Zhang,^{1,2} Li Tao,³ Wenkai Cheng,⁴ Jianhua Liu,^{1,2,*} and Zhongping Chen⁵

¹Department of Optical Science and Engineering, Key Laboratory for Micro and Nanophotonic Structures (Ministry of Education), Fudan University, Shanghai 200433, China

²Shanghai Ultra-Precision Optical Manufacturing Engineering Center, Fudan University, Shanghai 200438, China

³Department of Electrical Engineering, Stanford University, Stanford, California 94305, USA

⁴KLA-Tencor Semiconductor Equipment Technology (Shanghai) Co. Ltd., Shanghai 201203, China

⁵Beckman Laser Institute, Department of Biomedical Engineering, University of California, Irvine, California 92612, USA

*Corresponding author: jhliu@fudan.edu.cn

Received 2 June 2014; revised 1 August 2014; accepted 2 August 2014;
posted 5 August 2014 (Doc. ID 212473); published 4 September 2014

In spectral domain interferometry, the interference signal generated by directly reflected waves from the two surfaces of a sample plate under test is greatly enhanced by the blockage of those light waves reflected by the two arm mirrors in the Michelson interferometer. This sample surface-reflected interference signal, being the optical path length of the plate, is therefore identifiable directly from the Fourier-transformed interference spectrum. Consequently, the group refractive index and physical thickness of the plate can be obtained simultaneously without any prior information of them. Moreover, subsequent *in situ* angular scanning on the interference spectra helps to retrieve the wavelength-dependent phase refractive index and first-order dispersion. The order of magnitude of the relative error for the group refractive index is 10^{-4} , while that for the phase refractive index and the physical thickness is 10^{-3} . © 2014 Optical Society of America

OCIS codes: (120.3180) Interferometry; (120.4290) Nondestructive testing; (120.4530) Optical constants; (170.4500) Optical coherence tomography.
<http://dx.doi.org/10.1364/AO.53.005906>

1. Introduction

Accurate measurements of the optical parameters, such as physical thickness and refractive index of optical plates, are important in research and practical applications [1,2]. The interferometric method, in general, measures the optical path length (OPL) in a sample [3], which is a coupled quantity of refractive index and physical thickness. In order to retrieve the two parameters individually, many groups have proposed their methods [4–12]. Based on optical coherence tomography (OCT) or low coherence interferometry

(LCI), Wang *et al.* [4], Hirai and Matsumoto [5], and Cheng and Liu [6] measured the group refractive index and physical thickness of their samples in the time domain. Na *et al.* [7], Park *et al.* [8], and Maeng *et al.* [9] measured these parameters in the spectral domain (SD) or Fourier domain. Combining confocal optics, Maruyama and co-workers [10,11] and Kim *et al.* [12] measured an additional parameter, the phase refractive index, in the time domain.

Because of no mechanically scanning part, it is evident that the measurements of those optical parameters in the spectral domain is advantageous over that in the time domain; therefore, the spectral domain method has been dominant in the fields of OCT and LCI in recent years [13,14].

In SD LCI, the OPL is usually obtained by the interference of light reflected from the sample surfaces and from the mirror in the reference arm in a conventional Michelson interferometer, with subsequent subtraction of the two peaks in the Fourier-transformed interference spectrum [7]. In fact, getting the OPL with intermediate by the reference mirror is actually unnecessary. Interference implying OPL can actually happen simultaneously between light reflected from the two surfaces of the sample under test, which can be used to identify the value of the OPL directly. However, in the conventional SD scheme of Michelson interferometry, the signal of this surface-reflected interference (SRI) is usually too low to be noticeable due to the lower reflectance of the sample surfaces.

On the other hand, it is clear that the group refractive index, n_g , is referred to the phase delay experienced by a wave packet of low coherence length or a short optical pulse, which transmits through the sample plate at normal direction. If the direction of incidence is not in the normal, the phase refractive index, n_p , which is wavelength dependent, has to be used in order to describe the refractive propagation of the multiwavelength wave packet. Therefore, it is highly desirable to distinguish the phase refractive index (n_p) from the group refractive index (n_g) when dealing with problems of light wave propagation. It is shown that simultaneous measurements of parameters, including phase refractive index and dispersion, in SD interferometry have not been reported yet.

In this paper, we propose a simple method based on SD LCI with an evidently enhanced signal of OPL, which is formed by the interference of the light waves collinearly reflected from the front and rear surfaces of sample plates under test, so that the OPL can be read out directly other than by subtracting of two relative peaks [7]. Consequently, the physical thickness and group refractive index of transparent optical plates can be obtained simultaneously. With the obtained value of the thickness of the plate, phase refractive index and dispersion can be measured *in situ* with the same apparatus with additional angular scanning.

2. Method

Figure 1 shows the experimental setup, which consists of a light source with low coherence length, a beam splitter used to separate reference and sample arm beams, a rotation stage on which the sample plate under test is positioned with an adjustable mount in three dimensions, two switchable light shutters controlling the beams reaching the two mirrors behind, and an achromatic lens focusing light into an optical fiber, which couples the light into an optical spectrum analyzer (OSA).

LCI is commonly used to measure physical thickness d and group refractive index n_g of optical plates. To do that two independent relations between d and n_g have to be worked out. The first one is the value of $(n_g - 1) \cdot d$, which can be obtained from spectral interference of the two mirror (SM and RM) reflected

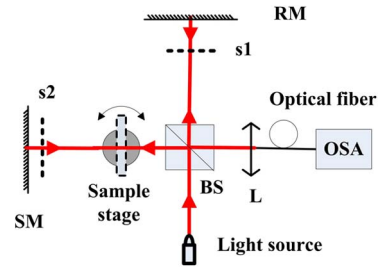


Fig. 1. Schematic of experimental setup. BS, beam splitter; OSA, optical spectrum analyzer; SM, sample mirror; RM, reference mirror; L, achromatic lens; s1 and s2, switchable shutters.

beams with and without the sample plate positioned in the sample arm [7–9,15]. The second one is the value of $n_g \cdot d$, the OPL, which is usually obtainable from the interferences of light reflected from sample surfaces and the reference mirror [7–9].

Instead, in our method, $n_g \cdot d$ could be obtained directly from a single interference spectrum formed by light reflected from the front and rear surfaces of the plate, rather than intermediate by the reference mirror as usually done in conventional Michelson interferometry. We call this SRI. Usually the SRI signal is very low compared with those interference signals correlated with the reference mirror. In our method, the enhancement of the SRI signal can be implemented by blocking the beams coming from the two mirrors by two switchable shutters setting in the two arms, as denoted by s1 and s2 in Fig. 1.

Given OPL and $(n_g - 1) \cdot d$ carried out, the group refractive index, n_g , and the physical thickness, d , can then be simultaneously obtained. Moreover, as the physical thickness, d , is obtained, the phase refractive index, n_p , is retrievable by angular scanning *in situ* with the same measurement system.

Modeling the light propagation, we denote the angle of incidence on the surface of the plate as α . Then the single pass optical path difference (OPD), Δ_{opd} , before and after the sample plate is put in the sample beam path and can be expressed as [16]

$$\Delta_{\text{opd}}(\alpha) = \left(\sqrt{np^2 - \sin^2 \alpha} - \cos \alpha \right) \cdot d, \quad (1)$$

where the refractive index of air is taken as 1.0.

For partially coherent light beams, the light intensity interfered between beams reflected from the reference arm (I_R) and that from the sample arm (I_S) at wavelength λ can be expressed as [17]

$$I = I_R + I_S + 2\gamma \sqrt{I_R I_S} \cos[k \cdot 2\Delta_{\text{opd}}(\alpha) + \varphi_0], \quad (2)$$

where γ denotes the parameter that is called degree of coherence (DOC) [17]; $k = 2\pi/\lambda$ is the wave vector; and λ is the wavelength in free space. φ_0 represents the initial phase difference.

Experimentally measuring the interference spectra within a certain range of incident angles, the interference intensity at wavelength λ , $I(\lambda, \alpha)$, can be

fitted as a function of the incident angle α . Thereafter, the phase refractive index at that wavelength can be retrieved.

It is known that the relationship between n_g , n_p , and the first-order dispersion $dn_p/d\lambda$ is as [18]

$$n_g = n_p - \lambda_c (dn_p/d\lambda)_{\lambda_c}, \quad (3)$$

where λ_c is the central wavelength of the light source. Therefore, the value of the first-order dispersion can then be calculated at the central wavelength with obtained values of n_g and n_p .

3. Experiments and Results

In our experiment, the light source was a simple GaAs laser driven just below its threshold voltage. Its output spectrum was centered at 648 nm with 10 nm full width at half-maximum (FWHM) bandwidth. The OSA was of a model AQ-6315A (ANDO Electric Co., Ltd.) working at 0.05 nm resolution. The first sample under test was a simple slide glass.

To obtain the value of $(n_g - 1) \cdot d$, first the two shutters were open in the two light arms, and the interference spectra before and after the sample plate was put in the sample arm were measured, which are shown as insets (a) in Figs. 2 and 3, respectively. Normalized spatial spectra, which were Fourier transformed on the measured intensity spectra, are shown in Figs. 2(b) and 3(b), respectively. In Fig. 2(b), the higher peak denoted as “RS” results from the interference of light beams reflected from the reference and sample mirrors without the sample plate in the path, whereas in Fig. 3(b), the “RSs” denoted peak is the shifted signal of “RS” due to the presence of the sample plate in the beam path. The single pass OPD then corresponds to that shift of peak positions in spatial spectra, i.e., $(n_g - 1) \cdot d = \text{RSs} - \text{RS}$.

In order to obtain the value of $n_g \cdot d$, the two shutters were set closed preventing light reflections on the sample mirror (SM) and the reference mirror (RM), so that light beams coupled into the OSA were reflected from the front and rear surfaces of the sample plate only. The measured spectrum and its normalized FFT spatial spectrum are shown in Figs. 4(a) (inset) and 4(b), respectively. It is the peak denoted by “SRI” in Fig. 4(b), that resulted from the interference of light reflected at the front and rear

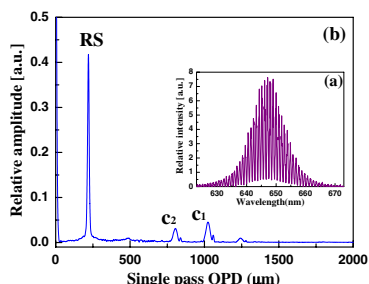


Fig. 2. (a) (Inset) Interference spectrum recorded without a sample in the beam path and (b) its normalized Fourier-transformed spatial spectrum. The sample was a simple slide glass.

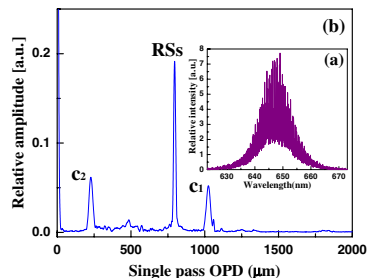


Fig. 3. (a) (Inset) Interference spectrum recorded with a sample in the beam path and (b) its normalized Fourier-transformed spatial spectrum. The sample was a simple slide glass.

surfaces of the sample plate. So that the OPL is given by the reading of the SRI peak from the horizontal axis of Fig. 4.

A noticeable feature of the SRI signal in Fig. 4 is its prominent amplitude, which is more than 20% of the normalized spatial spectrum peak, and is at least 20 times enhanced compared with that in the corresponding position (around 1600 μm) in Fig. 3. Without elimination of the arm mirror reflected waves, the SRI signal is usually too low (less than 1%) to be identifiable in the conventional SD LCI, Fig. 5 of [7], for example.

Small peaks, denoted by “ c_1 ” and “ c_2 ” in Figs. 2–4, came from cavity reflections in the light source, which are explained qualitatively in the Discussion part.

Quantitatively, spatial positions of peaks in Figs. 2, 3, and 4 for the slide glass sample read as $\text{RS} = 220.1 \pm 0.3 \mu\text{m}$, $\text{RSs} = 795.8 \pm 0.9 \mu\text{m}$, and $\text{SRI} = 1652 \pm 1 \mu\text{m}$, respectively, where standard error bars came from repeated measurements. Therefore, group refractive index n_g and physical thickness d were calculated as $n_g = 1.535 \pm 0.001$ and $d = 1076 \pm 1 \mu\text{m}$, respectively. The value of n_g of our sample is comparable with that of the B270 sample [12], where though the working wavelength referred was 814 nm.

For comparison purposes, the physical thickness of the slide glass was also measured with a mechanical caliper as $1087 \pm 3 \mu\text{m}$. The relative discrepancy of about 1% between the two independent methods was thus acceptable. The second sample in our experiment was an ITO-coated glass square. The calipered

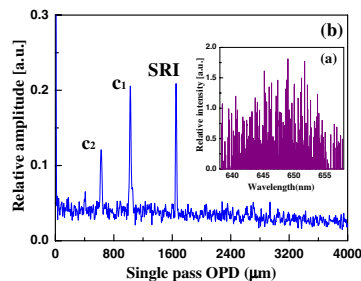


Fig. 4. (a) (Inset) Interference spectrum from surface reflections of the sample plate (SRI) and (b) its normalized Fourier-transformed spatial spectrum. The sample was a simple slide glass.

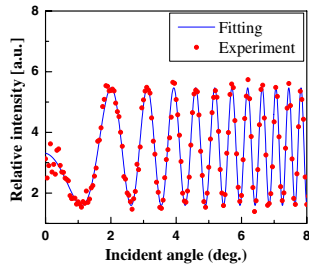


Fig. 5. Measured interference intensity (red dots) at wavelength of 648 nm and theoretical fitting (blue line) as function of angle of incidence. The sample was a simple slide glass.

thickness of the ITO glass was $713 \pm 2 \mu\text{m}$, whereas the value obtained by LCI was $709.1 \pm 0.6 \mu\text{m}$, resulting in a deviation of only 0.6%.

Without removing the sample from the mount, the phase refractive index was measured with the same system (*in situ*) by scanning the incident angle within a certain range as the rotation of the sample stage. Interference spectra at each small increment of incident angle (0.05 deg in the experiment) were detected. Selected from those spectra, the intensity of light at the central wavelength 648 nm as a function of the angle of incidence is plotted in Fig. 5 for the slide glass sample. It can be seen that, with the obtained thickness d of the sample, the theoretically fitted line (blue) according to Eq. (2) with the least-squares method, goes very well with the experimental data points, giving rise to a consistent result of phase refractive index for the slide glass sample, $n_p = 1.514 \pm 0.003$, compared with published data [19]. Actually, the value of this parameter for the slide glass varied in the literature, ranging from 1.51 to 1.522 [19–21], depending probably on the glass composition. Data fitting is simply implemented by adoption of library function “lsqcurvefit()” in Matlab v.R2012. Interference intensities for other wavelengths for angular fitting were also obtainable in the whole measured spectral bandwidth.

Dispersion was thereafter obtained according to Eq. (3) as $dn/d\lambda = -0.031 \pm 0.004 \mu\text{m}^{-1}$. Although our source spectrum is relatively narrow, a meaningful material dispersion spectrum could be retrieved with our method if the spectrum of the light source is wide enough.

Those obtained parameters for the slide glass sample, as well as the second sample, an ITO-coated glass plate, are all tabulated in Table 1. Standard error for each parameter was calculated by data of repeated measurements. It can be seen that the

order of magnitude of relative error for the group refractive index is 10^{-4} , while that for the phase refractive index and the thickness is around 10^{-3} , and that for the first-order dispersion is 10^{-1} .

4. Discussion

It can be seen in Figs. 2–4 that the peak denoted with “ c_1 ” has a fixed spatial position, at about $1020 \mu\text{m}$. It exists even for the spectrum of the light source without going through the measurement system. It is consistent with the cavity length of a common GaAs laser of about 0.3 mm and with the refractive index of about 3.35 for GaAs. Therefore, it is attributed to the interference between the wave packets of successive round-trip reflection of the laser output. Thus, the light source consists mainly of two successive wave packets with a stronger one in front and a weaker one lagging behind with a separation distance of 2 times of the “ c_1 ” mode.

The Michelson interferometer splits the beam into reference and sample arms with a relative delay between the separated wave packets. Therefore, the measured spectrum is an interference spectrum with at least four wave packets from the two arms. Higher-order reflected waves could be neglected. The modes “ c_2 ” comes from the interference between the main packet of one arm with relative delay and that of the minor packet in the other arm. The relative amplitudes of these interference modes in the spatial spectrum are affected by DOC [17], the degree of coherence of the light source, and by the resolution of the OSA.

Given these results obtained, it is evident that our method allows for quantification of multiple optical parameters of flat materials, such as optical windows and polymer films. Compared with the method in [7], the key difference of our method lies in getting the value of the OPL of the plate, i.e., $n_g d$, by spectral interference of single path beams reflected from the surfaces of the sample itself, instead of by waves from the two-arm paths of the Michelson interferometer. With the elimination of those light waves reflected from the arm mirrors, SRI then gets greatly enhanced (at least 20 times) and allows us to “read” the value of $n_g d$ directly from a single peak (SRI in Fig. 4), instead of subtracting two peaks as conventionally done in [7].

The technical advantage of sample SRI is that it is immune to the environmental uncertainties (vibrations, turbulence, etc., as described in [7]) so that it is more stable compared with interference of waves coming from physically separated surfaces of mirrors

Table 1. Measured Multiple Parameters for Slide Glass and ITO Glass Samples at Central Wavelength 648 nm

Sample	Thickness (μm)			Group Index			Phase Index			Dispersion (μm^{-1})		
	d	err ^a	r ^b	n_g	err	r	n_p	err	r	$dn/d\lambda$	err	r
Slide	1076	1	0.0013	1.535	0.001	0.0006	1.514	0.003	0.0017	-0.031	0.004	0.14
ITO	709.1	0.6	0.0009	1.5365	0.0005	0.0003	1.512	0.002	0.0012	-0.038	0.004	0.11

^aStandard error.

^bRelative error.

and the sample. Therefore, our result could be very good with standard error of the order of 10^{-4} without additional stabilization aids.

Another advantage of our method over the conventional SD LCI is the separation of the correlations in obtaining the values for $n_g d$ and $(n_g - 1)d$. In our method, they correspond to two irrelevant interferences between the sample surfaces and between the mirrors in the two arms of the Michelson interferometer, respectively. Consequently, the two arm lengths of the Michelson interferometer can be extended synchronously to make free space for the sample stage, so that the sample in the sample arm can be put at any position as long as the optical path length difference (OPD) between the two arms is less than the measurable depth range (MDR) of the system [7,22].

Comparatively, conventional SD LCI requires the sample to be positioned very close to the mirror in the sample arm, because the three surfaces (sample surfaces and the mirror) in the sample arm have to be correlated with the reference arm mirror with restriction of the MDR, which made it impossible to change the incident angle [7]. Our design allows the sample to be able to rotate freely, so that the angle of incidence could be changed as needed. By means of this, the phase refractive index can be retrieved additionally *in situ* the same system without moving the sample to another measurement apparatus. This functional extendibility is not implementable in previously published SD methods.

Principally, getting data for n_p is separable from that for n_g and d provided that the thickness of the sample is known in advance. With no prior information on the thickness, one has to resort first to other methods or systems. However, our method can make a breakthrough in this situation. That is, without prior information on any of these three parameters, we can retrieve them accurately in the SD.

Additionally, n_p obtained in our method is wavelength resolvable, and so is the "dispersion." That is because intensities of all wavelengths in the experimental spectral band have been measured at each angular step. Figure 5 shows the typical variation of the interference intensity at 648 nm merely. If the bandwidth of the light source could be spanned in a wider range, the dispersion spectrum can be worked out.

The accuracy of our method with no special stabilization aid is comparable to those published methods in the SD [7,8]. It is restricted mainly by the quality of sample surfaces. From Table 1, it can be seen that the relative errors for all of the parameters for ITO glass are better than those of slide glass. This is because the slide glass surfaces were not as carefully processed as those of ITO.

5. Conclusion

Making use of SRI we were able to measure multiple parameters of transparent plates, which are the physical thickness, the group refractive index, the

phase refractive index and dispersion, in a simple system by means of SD LCI. SRI signal was greatly enhanced by eliminating the stronger light beams reflected by the two arm mirrors, so that it was prominent enough to be identified directly for OPL value. SRI can also be of help in reducing uncertainties in the measurements.

Because of the separation of the coherent correlations between the sample surfaces and the arm mirrors in the Michelson interferometer, the system flexibility, thus the functional extendibility, is considerably enriched.

The order of magnitude of the relative error for the group refractive index was 10^{-4} , while that for the phase refractive index and physical thickness was 10^{-3} .

This work is supported by the Shanghai Committee of Science and Technology with contract No. 11ZR1403600, and by the Key Laboratory Senior Visiting Scholarship of Fudan University.

References

1. M. Ohmi, Y. Ohnishi, K. Yoden, and M. Haruna, "In vitro simultaneous measurement of refractive index and thickness of biological tissue by the low coherence interferometry," *IEEE Trans. Biomed. Eng.* **47**, 1266–1270 (2000).
2. A. M. Zysk, S. G. Adie, J. J. Armstrong, M. S. Leigh, A. Paduch, D. D. Sampson, F. T. Nguyen, and S. A. Boppart, "Needle based refractive index measurement using low-coherence interferometry," *Opt. Lett.* **32**, 385–387 (2007).
3. A. F. Fercher, K. Mengedocht, and W. Werner, "Eye-length measurement by interferometry with partially coherent light," *Opt. Lett.* **13**, 186–188 (1988).
4. X. Wang, C. Zhang, L. Zhang, L. Wue, and J. Tian, "Simultaneous refractive index and thickness measurements of bio tissue by optical coherence tomography," *J. Biomed. Opt.* **7**, 628–632 (2002).
5. A. Hirai and H. Matsumoto, "Low-coherence tandem interferometer for measurement of group refractive index without knowledge of the thickness of the test sample," *Opt. Lett.* **28**, 2112–2114 (2003).
6. H. Cheng and Y. Liu, "Simultaneous measurement of group refractive index and thickness of optical samples using optical coherence tomography," *Appl. Opt.* **49**, 790–797 (2010).
7. J. Na, H. Y. Choi, E. S. Choi, C. Lee, and B. H. Lee, "Self-referenced spectral interferometry for simultaneous measurements of thickness and refractive index," *Appl. Opt.* **48**, 2461–2467 (2009).
8. S. Park, K. S. Park, Y. H. Kim, and B. H. Lee, "Simultaneous measurements of refractive index and thickness by spectral-domain low coherence interferometry having dual sample probes," *IEEE Photon. Technol. Lett.* **23**, 1076–1078 (2011).
9. S. Maeng, J. Park, B. O, and J. Jin, "Uncertainty improvement of geometrical thickness and refractive index measurement of a silicon wafer using a femtosecond pulse laser," *Opt. Express* **20**, 12184–12190 (2012).
10. M. Haruna, M. Ohmi, T. Mitsuyama, H. Tajiri, H. Maruyama, and M. Hashimoto, "Simultaneous measurement of the phase index and group indices and the thickness of transparent plates by low-coherence interferometry," *Opt. Lett.* **23**, 966–968 (1998).
11. H. Maruyama, S. Inoue, T. Mitsuyama, M. Ohmi, and M. Haruna, "Low-coherence interferometer system for the simultaneous measurement of refractive index and thickness," *Appl. Opt.* **41**, 1315–1322 (2002).
12. S. Kim, J. Na, M. J. Kim, and B. H. Lee, "Simultaneous measurement of refractive index and thickness by combining low-coherence interferometry and confocal optics," *Opt. Express* **16**, 5516–5526 (2008).

13. G. Li, P.-C. Sun, P. Lin, and Y. Fainman, "Interference microscope for 3D imaging with a wavelength-to-depth encoding," *Opt. Lett.* **25**, 1505–1507 (2000).
14. G. Li and Y. Fainman, "Analysis of wavelength-to-depth encoded interference microscope for three-dimensional imaging," *Opt. Eng.* **41**, 1281–1288 (2002).
15. Q. Xiao, J. Wang, S. Zeng, and Q. Luo, "A spectral interferometric method to measure thickness with large range," *Opt. Commun.* **282**, 3076–3080 (2009).
16. H. G. Yun, S. H. Kim, H. S. Jeong, and K. H. Kim, "Rotation angle measurement based on white-light interferometry with a standard optical flat," *Appl. Opt.* **51**, 720–725 (2012).
17. M. Born and E. Wolf, *Principles of Optics*, 7th ed. (Cambridge University, 2005), Sects. 10.4.1 and 10.4.4.
18. B. L. Danielson and C. Y. Boisrobert, "Absolute optical ranging using low coherence interferometry," *Appl. Opt.* **30**, 2975–2979 (1991).
19. K. B. Blodgett, "Properties of built-up films of barium stearate," *J. Phys. Chem.* **41**, 975–984 (1937).
20. K. E. Youden, T. Grevatt, R. W. Eason, H. N. Rutt, R. S. Deol, and G. Wylangowski, "Pulsed laser deposition of GaLaS chalcogenide glass thin film optical waveguides," *Appl. Phys. Lett.* **63**, 1601–1603 (1993).
21. P. E. Gaskell, H. S. Skulason, C. Rodenchuk, and T. Szkopek, "Counting graphene layers on glass via optical reflection microscopy," *Appl. Phys. Lett.* **94**, 143101 (2009).
22. Z. Ding, H. Ren, Y. Zhao, J. S. Nelson, and Z. Chen, "High-resolution optical coherence tomography over a large depth range with an axicon lens," *Opt. Lett.* **27**, 243–245 (2002).